The protocadherin Flamingo is required for axon target selection in the *Drosophila* visual system

Roger C Lee[1,5], Thomas R Clandinin[1,2,5], Chi-Hon Lee[1,4], Pei-Ling Chen[2], Ian A Meinertzhagen[3] & S Lawrence Zipursky[1]

Photoreceptor neurons (R cells) in the *Drosophila* visual system elaborate a precise map of visual space in the brain. The eye contains some 750 identical modules called ommatidia, each containing eight photoreceptor cells (R1–R8). Cells R1–R6 synapse in the lamina; R7 and R8 extend through the lamina and terminate in the underlying medulla. In a screen for visual behavior mutants, we identified alleles of *flamingo* (*fmi*) that disrupt the precise maps elaborated by these neurons. These mutant R1–R6 neurons select spatially inappropriate targets in the lamina. During target selection, Flamingo protein is dynamically expressed in R1–R6 growth cones. Loss of *fmi* function in R cells also disrupts the local pattern of synaptic terminals in the medulla, and Flamingo is transiently expressed in R8 axons as they enter the target region. We propose that Flamingo-mediated interactions between R-cell growth cones within the target field regulate target selection.

Neurons make precise patterns of synaptic connections in a step-wise fashion[1]. Extracellular signals that act as attractants or repellents are detected by growth cones and used to guide extending axons toward their targets. Such signals can act either at short range, via contact between the growth cone and the surface of cells along the pathway, or at long range, as gradients of attractants or repellents. In some systems, axons elaborate topographic maps. In the retinotectal system, for example, the formation of these maps is regulated by the spatially graded expression of membrane-bound repellents called EphrinAs on the surface of tectal cells, as well as by the graded distribution of EphrinA receptors called EphAs on the growth cones of retinal ganglion cells[2]. Several cell-surface proteins have been identified in both vertebrate and invertebrate systems that are crucial in forming precise connections after growth cones reach the target region. These include N-cadherin[3,4], Sidekick[5], MHC class-I proteins[6], *C. elegans* Syg-1[7], *Drosophila* Dscam[8] and vertebrate olfactory receptors[9]. In culture systems, both neuroligin/β-neurexin[10] and syn-CAM[11] have been shown to promote synapse formation.

Activity-dependent processes, especially in vertebrate systems, often refine or stabilize patterns of synaptic connections[12]. This has led to the view that initial patterns of connections, driven by genetically hardwired mechanisms, are relatively crude and are refined by activity-dependent events. Recent studies, however, challenge this view and raise the possibility that genetically hardwired mechanisms are essential for fine-scale determination of specificity[13,14]. To explore the molecular mechanisms regulating complex and precise patterns of synaptic connections, we investigated the formation of connections between a subclass of *Drosophila* photoreceptor neurons, R1–R6, and their targets.

The synaptic connections elaborated by R1–R6 neurons in the fly visual system provide a striking example of the complexity and precision of neuronal connectivity[15,16]. As a consequence of their arrangement within an ommatidium, each of the six cell types views a different point in space. Each also connects to a different group of lamina neurons, forming a module called a cartridge. The cartridges chosen by R1–R6 from the same ommatidium are arranged in a precise spatial pattern. As a further consequence of the geometric relationship between ommatidia, a single R1–R6 neuron in one ommatidium views the same point in space as five others, one in each of five neighboring ommatidia[17]. Remarkably, the axons of the six R1–R6 cells that view the same point in space connect to neurons in the same cartridge.

R1–R6 target selection involves a precise rearrangement of photoreceptor growth cones within the lamina[16]. Although R1–R6 axons from the same ommatidium project to different target cartridges (**Fig. 1**), they initially extend into the lamina as a single fascicle also comprising R7 and R8 from the same ommatidium, and they terminate at a common site. At that site, R1–R6 growth cones recognize a 'stop' signal produced by lamina glial cells[18,19], whereas R7 and R8 axons extend into the medulla. Initially, R1–R6 growth cones from a single ommatidium form a compact cluster at the distal surface of the lamina. Following a stereotyped sequence of morphological changes, each growth cone subsequently projects to a different lamina target[16] during a process of lateral sorting that is required for selection of the appropriate target cartridge. Synapses form much later[16]. These pat-

[1]Department of Biological Chemistry, David Geffen School of Medicine at UCLA, Howard Hughes Medical Institute, Box 951662, Los Angeles, California 90095-1662, USA. [2]Department of Neurobiology, Stanford University School of Medicine, Sherman Fairchild Science Building, 299 W. Campus Drive, Stanford, California 94305, USA. [3]Neuroscience Institute, Life Sciences Centre, Dalhousie University, Halifax, Nova Scotia B3H 4J1, Canada. [4]Present address: NICHHD/NIH, Building 18T, Rm. 106, MSC 5431, Bethesda, Maryland 20892, USA. [5]These authors contributed equally to this work. Correspondence and requests for materials should be addressed to S.L.Z. (zipursky@hhmi.ucla.edu).

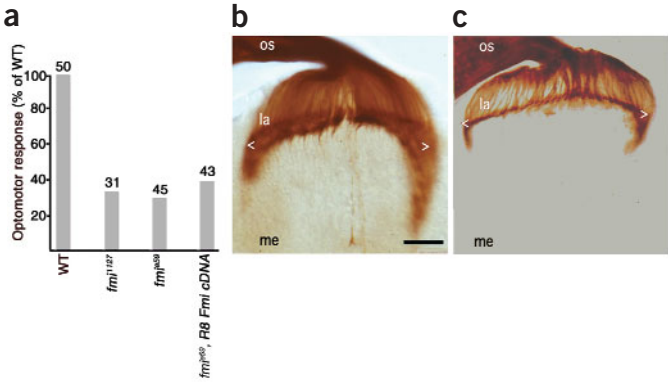

Figure 1 Mosaic *fmi* animals show defective optomotor response but normal R1–R6 target layer specificity. (**a**) The optomotor response of *fmi* mutant flies is defective. The numbers above each bar indicate the number of flies tested for each genotype. Although R8 projections are affected in *fmi* mutants (Results and **Fig. 5**), targeted expression in R8 did not rescue the optomotor phenotype. (**b**,**c**) R2–R5 axons were visualized selectively with a *ro-tau-lacZ* reporter to assess targeting to the lamina in third-instar optic lobes. Like wild-type R2–R5 axons (**b**), axons of *fmi* mutant R2–R5 neurons (**c**) terminated in the lamina (la). os, optic stalk; me, medulla; brackets (<>) demarcate the nascent lamina neuropil. Scale bar, 20 μm.

terns of connections are formed before the expression of rhodopsin and are therefore independent of light-evoked activity; the role of spontaneous activity has not been critically evaluated. In previous genetic studies, we have shown that the extension of growth cones to cartridges in the developing lamina relies on N-cadherin[4] and the tyrosine phosphatase Lar[15]. Based on protein expression patterns and phenotypic analyses on R7 targeting[4] and more recent studies in the olfactory system (T. Hummel and S.L.Z., unpublished data), we propose that N-cadherin promotes interaction between R1–R6 growth cones and their targets or stabilizes these interactions.

While it is obvious that interactions between R-cell growth cones and lamina target neurons are essential for targeting specificity, it is surprising that interactions between R1–R6 cells are essential for appropriate target selection. The stereotyped sequence of morphological changes revealed by electron microscopy led to the view[16] in the early 1970s that interactions between growth cones were essential to the appropriate sorting, and hence targeting, of R1–R6 growth cones to specific cartridges. More recently, our genetic studies[20] have shown that when specific subclasses of R1–R6 neurons are removed, the remaining R1–R6 neurons select incorrect cartridges, indicating that interactions between R cells are, indeed, essential for target selection.

Here we show that Flamingo, a cadherin-related cell surface protein[21,22], is required for R1–R6 axons to select appropriate targets in the lamina. The gene encoding Flamingo is centrally involved in mediating interactions between epithelial cells that regulate planar cell polarity[21,22], Flamingo protein promotes cell aggregation in culture[21], and genetic studies show that *fmi* is involved in regulating dendritic patterning[23]. In the present study, we found that in *fmi* mutants, R1–R6 axons extend to inappropriate targets in the lamina and form abnormal cartridges containing variable numbers of R1–R6 terminals. R1–R6 axons still formed morphologically normal synapses in inappropriate targets. Flamingo was also required for the appropriate sorting of R8 axons to specific targets in the medulla. On the basis of these mutant phenotypes and the dynamic expression patterns of Flamingo in R-cell axons, we

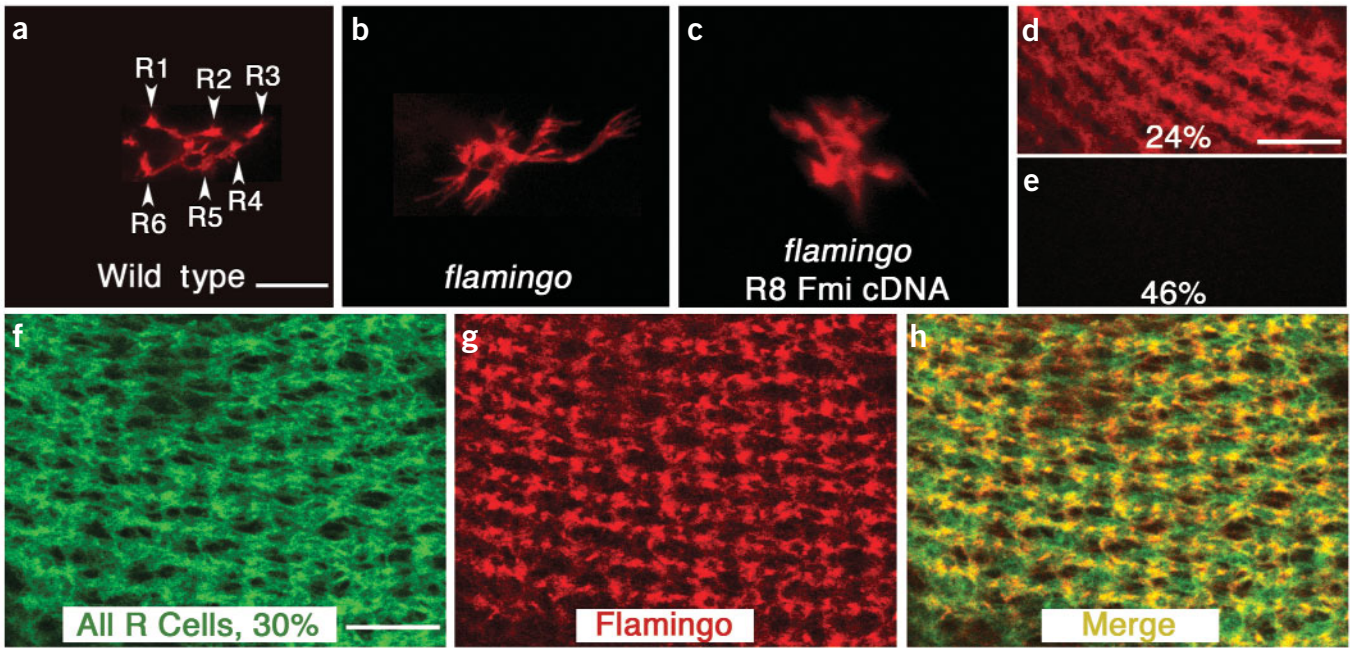

Figure 2 The *flamingo* gene is required for R1–R6 axons to choose the appropriate pattern of targets in the developing lamina and is expressed in R1–R6 growth cones. (**a**–**c**) DiI-labeled projections of photoreceptor axons from single ommatidia at 40% of adult development, at the onset of cartridge assembly. (**a**) R1–R6 axons in control animals extend outward in an invariant pattern, each axon identified by its characteristic trajectory. (**b**) R1–R6 axons in *fmi* mutants extend in an abnormal, more diffuse pattern. (**c**) Targeted expression of *fmi* in R8 does not rescue mutant R1–R6 axons projecting into a heterozygous target; defects in R1–R6 do not result from non-autonomous defects in R8 (Results and **Fig. 5**). (**d**–**h**) Anti-Flamingo labeling (red) in developing lamina at 24% (**d**), 46% (**e**) and 30% (**g**,**h**) of adult development. (**f**,**h**) A pan-photoreceptor axonal marker, pGMR–GFP (green) visualized either alone (**f**) or merged (**h**) with anti-Flamingo at 30%. Scale bars, 10 μm. See **Supplementary Fig. 1** for a diagram representing the sorting defects documented in this figure and in **Fig. 3**.

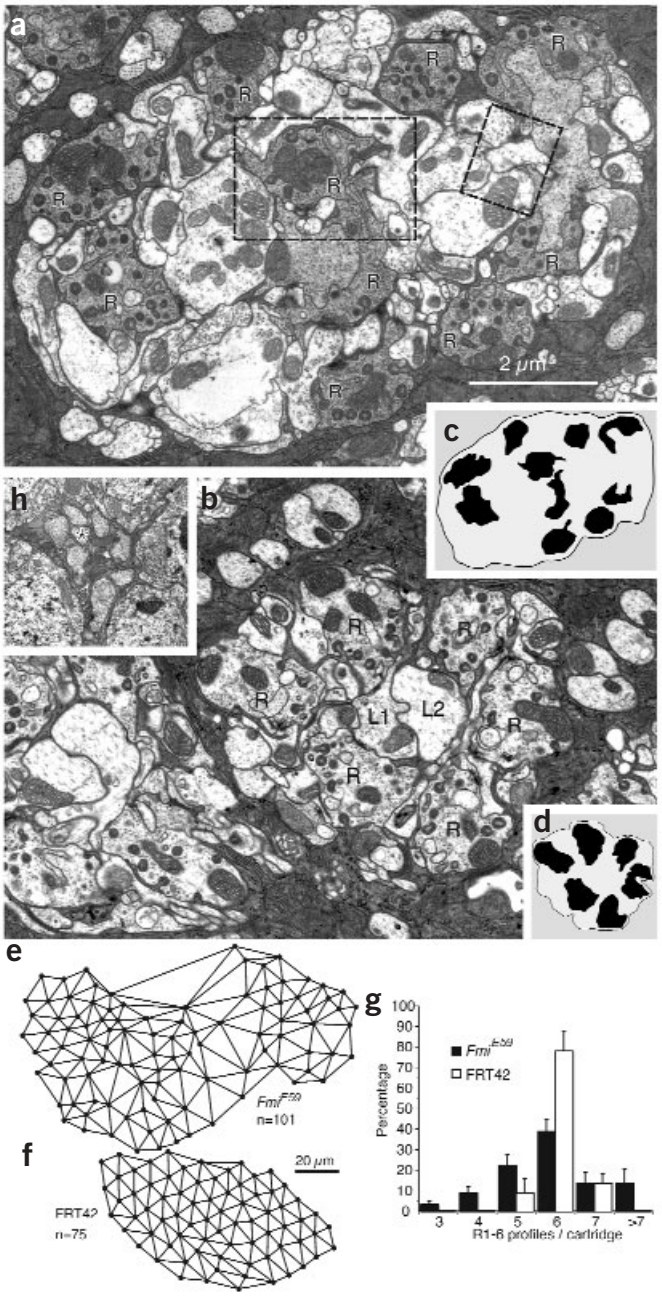

Figure 3 Functional *flamingo* is required for assembly of synaptic units, called cartridges, in the lamina. (**a**,**b**) Comparison of axonal composition of *fmi* mutant (**a**, representative mutant cartridge with ≥10 R1–R6 terminals (R); wild-type cartridges in **b**). Ultrastructure appears as in wild type[27], and synapse numbers are also similar[28] (data not shown). The cytoplasm of mutant R1–R6 axons is darker than wild-type and control cartridges. (**b**) Control FRT42 cartridge with six terminals (R) encircling axon profiles of lamina monopolar cells L1 and L2, at the same magnification for comparison with (**a**). (**c**,**d**) Schematic representations of the cartridge composition in mutant (**c**) and control (**d**), showing R1–R6 terminals as dark profiles. (**e**,**f**) Array of lamina cartridges beneath *fmi* mutant (**e**) and control (**f**) eyes. Centers of cartridge profiles are connected by DeLaunay triangulation, giving a visual impression of their array. Many mutant cartridge profiles (as in **a**) are large and amorphous, lack circularity and distort the array. (**g**) The number of R1–R6 terminals per cartridge profile beneath *fmi* mutant and control eyes. Control laminas generally have 6 terminals; 5 and 7 profiles arise from confluence or branching of terminal profiles, respectively; some mutant cartridges have more terminals and are hyperinnervated at the expense of those with fewer. (**h**) Axon bundle in the lamina cortex, comprising eight photoreceptor axons, one of which (probably R8, *) lies at the center in a characteristic pattern resembling those of R1–R8 from a single wild-type ommatidium.

propose that Flamingo mediates specific interactions between afferents that are crucially involved in R-cell target selection.

RESULTS

To identify proteins that regulate R1–R6 targeting, we conducted a screen for mutations affecting the optomotor response, a behavior requiring correct R1–R6 function[24]. In this screen, we tested genetically mosaic animals in which the eye was homozygous mutant and the target was not[25]. Two alleles of *fmi* were isolated (**Fig. 1a**). To assess the functional requirement for *fmi* in photoreceptors, we generated genetic mosaic animals using the FLP/FRT system in which the FLP recombinase is expressed under the control of the *eyeless* promoter (*ey-FLP*). In these animals, virtually all R cells are made homozygous mutant[25]. As in wild type, *fmi* mutant R1–R6 axons in such genetically mosaic animals terminated in the lamina (**Fig. 1b**,**c**). Unlike wild type, however, their growth cones selected as synaptic targets lamina neurons that were in inappropriate locations, as assessed by DiI labeling experiments in developing pupae ($n = 14$; **Fig. 2b**). The penetrance of the phenotype was 100%, and the expressivity ranged in severity from complete loss to moderate disruption of the normal pattern of projections. There is no overlap between this phenotype and the R1–R6 targeting phenotypes previously described for *N-cadherin*[4] and *Lar*[24] mutants; Flamingo thus acts at a different step in target selection. Although small clones of mutant cells are found within lamina target neurons in mosaics generated using *ey-FLP* (P. Garrity, MIT, and I. Salecker, NIMR, personal communication), the complete penetrance of the phenotype indicates that it must be the loss of *fmi* function in R cells, rather than in their targets, that disrupts targeting.

Flamingo, like other cadherins, mediates homotypic cell adhesion[21]. To assess whether Flamingo mediates interactions between R1–R6 growth cones or between these growth cones and their targets, we characterized the pattern of Flamingo expression during target selection. Flamingo protein was transiently and dynamically expressed on R1–R6 growth cones during this period. At 24% of pupal development, Flamingo was expressed strongly on R1–R6 axons (**Fig. 2d**). Weak expression on lamina neuron cell bodies was also observed. By 30% of pupal development, Flamingo was expressed unequally in R1–R6 growth cones within the lamina plexus, as compared with uniform growth cone expression of the pan photoreceptor-specific marker, GMR–GFP (**Fig. 2f**,**g**). One likely explanation for this pattern is that specific subsets of R1–R6 growth cones express relatively high levels of Flamingo protein, while other subsets express little, if any. At the same stage, lamina neurons were almost entirely devoid of Flamingo expression, although in some preparations, a few scattered lamina cell bodies were labeled. Since all *fmi* mutant R cells showed targeting phenotypes, this very limited expression of Flamingo within the target field is unlikely to be of functional significance. By 46% of pupal development, Flamingo was no longer detected in photoreceptor axons and their growth cones (**Fig. 2e**). In contrast, N-cadherin is strongly expressed on both R1–R6 cell axons and on their lamina target neurons throughout development[4]. On the basis of these and other observations, we previously proposed that N-cadherin mediates interactions between photoreceptor growth cones and their targets. The dynamic and highly restricted expression of Flamingo, a homophilic cell adhesion molecule, on R1–R6 growth cones supports the view that Flamingo is directly involved in mediating interactions between R1–R6 growth cones that are required for target selection.

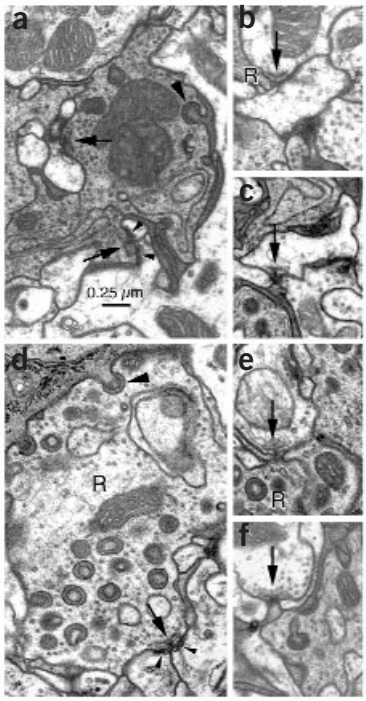

Figure 4 Synapses in laminas innervated by mutant photoreceptors do not differ from those in control laminas. (**a**–**c**) Synapses in cartridges innervated by *fmi* mutant R1–R6 terminals, shown at the same magnification. Scale bar in **a**, 0.25 μm. (**a**) Afferent tetrad synapses (arrows) formed by mutant R1–R6 terminals, from area within box in **Fig. 2a**. Synaptic organelles, such as capitate projection (arrowhead) and postsynaptic cisternae (small arrowheads), are structurally normal. (**b**) Feedback synapse (arrow) onto R1–R6 terminal (R) from unidentified element, probably L2 but possibly either L4 or a lamina amacrine cell, from area within box in **Fig. 2a**. (**c**) Other lamina synapse (arrow), probably between monopolar cells. (**d**–**f**) Corresponding synapses from cartridges innervated by control R1–R6 terminals shown at the same magnification and with the same labeling as (**a**–**c**). (**d**) Tetrad synapse. (**e**) Feedback synapse. (**f**) Synapse between lamina neurons.

To determine whether sorting defects observed during development resulted in cartridges of abnormal composition, we examined the arrangement of these in the adult lamina using electron microscopy (**Fig. 3a–d**). The cartridge array was markedly disrupted in genetically mosaic animals generated using *ey-FLP* (**Fig. 3e,f**). Many terminals innervated large cartridges, whereas others were smaller than wild type. To identify mis-sorting of R1–R6 terminals into the target cartridges, we counted the number of R1–R6 terminals within individual cartridge cross-sections. Provided each R1–R6 terminal innervates only a single cartridge, a mis-sorted terminal would deplete the correct cartridge's normal complement of 6, and increase that of another cartridge, to yield cartridge complements of 5 and 7, respectively. This assumes only that such a redistribution is not exactly offset by a complementary mis-sorting of another terminal, that is, that no consistent pattern of exchanging terminals occurred. The number of mutant terminals in each cartridge ranged from 3 to more than 15, compared with the normal number of 6–8 (see **Fig. 3** legend) in wild-type animals[16] (**Fig. 2g**; also compare **Fig. 2a** and **b**). Some terminals were dark and filled with synaptic vesicles, whereas others were paler, with fewer vesicles and lacking capital projections, or glial invaginations into the terminals[26]. Despite these differences and the abnormalities in sorting, the chief output synapses, or tetrads, elaborated by mutant R1–R6 cells had normal presynaptic organelles with a total of four postsynaptic elements, as traced through serial sections of 12 different synapses (**Fig. 4a,d**). As in wild type[27,28], feedback synapses onto mutant R1–R6 terminals, as well as other lamina synapses, were also present (**Fig. 4b,e**). The number of tetrad profiles was about 30% larger than in control terminals, but this difference was not significant ($P = 0.125$, *t*-test); mutant terminal size and the number of capitate projection profiles did not differ significantly from control values. These observations establish that *fmi* is necessary to sort R1–R6 axons to appropriate cartridge targets but that, once there, it is not required for synapse formation. These findings are consistent with studies in the house fly where mis-sorted wild-type axons induced by heat-shock treatment formed morphogically normal synapses[29].

Although the simplest interpretation of the data is that Flamingo mediates interactions between R1–R6 growth cones within the target region, we considered the possibility that Flamingo could affect these interactions only indirectly. Defects in projections could, for example, reflect disruptions in the polarity of the ommatidium[30,31], or an earlier role in R8, or defects in fascicle ordering before reaching the lamina target. A series of studies argue against these possibilities. First, the projection defects seen in *fmi* mutants are strikingly different from those seen in *frizzled* and *spiny legs*[20]—two mutants that show planar cell polarity defects in the eye similar to *fmi*[30,31]. Whereas the orientation of the projection pattern in *frizzled* and *spiny legs* largely reflects the orientation

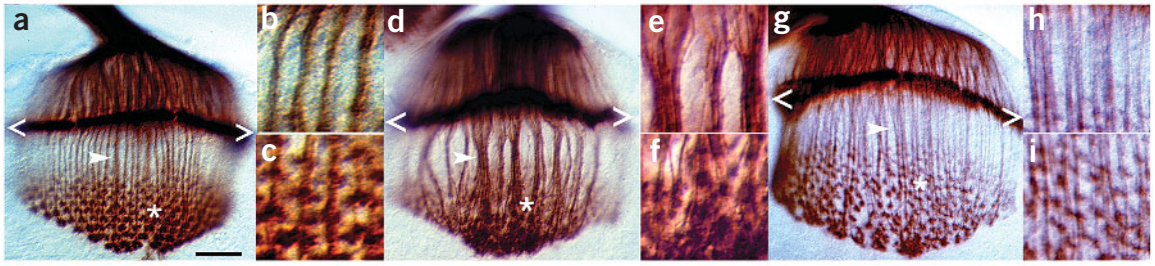

Figure 5 Functional *flamingo* is required in R8 for elaboration of precise array in the medulla. R-cell axon projections in eye–brain complexes of different genotypes immunolabeled with mAb24B10. (**a**–**c**) Wild-type R7 and R8 axons form uniform bundles (arrowhead in **a**; magnified in **b**), and their growth cones create a regular array of terminals in the developing medulla neuropil (asterisk in **a**; magnified in **c**). (**d**–**f**) *fmi* mutant R7 and R8 axons projecting into non-mutant medulla form thicker bundles than controls (arrowhead in **d**; magnified in **e**) between lamina and medulla layers and have a disrupted array of R8 terminals in the medulla (asterisk in **d**; magnified in **f**). (**g**–**i**) *fmi* mutant R-cell axons with R8-specific expression of wild-type *fmi* projecting into non-mutant targets. Local bundling defects in R8 fascicles are reduced (arrowhead), the fascicles are spaced more regularly (**h**), and the growth cones are not clumped (asterisk in **g**; magnified in **i**). Brackets in **a**, **d** and **g** demarcate the nascent lamina. Scale bar, 20 μm.

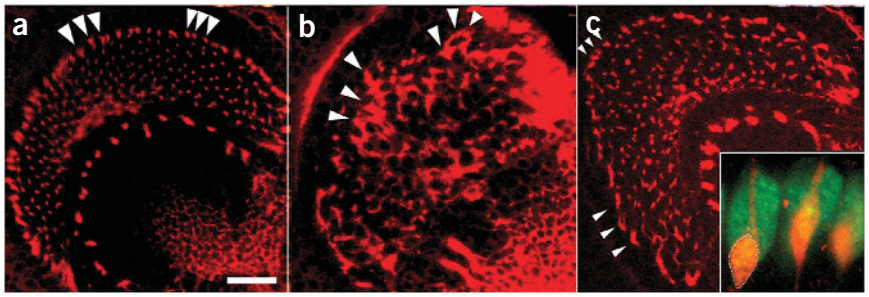

Figure 6 *flamingo* is required in R8 to form a smooth topographic map along the dorsoventral axis. R-cell axon projections in eye–brain complexes of different genotypes immunolabeled with neuron-specific anti-HRP coupled to Cy3 fluorophore. *En face* views of the R-cell axon bundle array, from the outside looking in, in a plane slightly above and parallel to the lamina. (**a**) Regular spacing of wild-type R-cell terminals as they enter the medulla target region. (**b**) Disrupted retinotopic array of *fmi* mutant R-cell axons projecting into a largely wild-type target. The disruption is particularly evident among the youngest, most anterior, clumped axon bundles at the outer edge of the crescent (arrowheads). (**c**) R8-specific expression of *fmi* using the Gal4 driver 109(2)68 Gal4 (ref. 33) restores the topographic order in *fmi* mutant mosaic animals. Note the regular spacing of axons along the outer edge of the crescent (arrowheads). Inset, expression pattern of 109(2)68 Gal4 in a single R8 cell within each ommatidium, as visualized by UAS-driven expression of cytoplasmic β-galactosidase. R8 occupies a characteristically basal-most position in the ommatidial cluster. Other R cells in the ommatidial cluster are stained by the pan-neuronal marker anti-HRP. Scale bar, 20 μm.

of the cells in the eye (and is frequently reversed along the dorsoventral axis by inversion of the ommatidium), the relative pattern of targets chosen by R1–R6 from a single ommatidium in these mutants is indistinguishable from wild type[20]. Second, the R1–R6 defects in *fmi* mutants are not a secondary consequence of defects in R8, as targeted expression of an *fmi* cDNA using the *Gal4–UAS* system[32,33] rescued the R8 targeting phenotype (**Fig. 5**) but did not rescue defects in R1–R6 target selection (**Fig. 2c**). Finally, electron micrographs showed that the composition of individual R1–R8 axon bundles above the lamina are indistinguishable from those in wild type (**Fig. 3h**), indicating that all defects in target selection must arise from defective sorting at the lamina surface rather than as a secondary consequence of aberrant R1–R8 fasciculation into bundles of abnormal composition.

Does Flamingo mediate interactions between other growth cones, or is its function restricted to sorting mechanisms required for R1–R6 connections? In our initial characterization of the *fmi* phenotype, we observed that *fmi* is also required to form precise retinotopic projections of R7 and R8 growth cones in the medulla. In developing third-instar eye–brain complexes or in adults labeled with monoclonal antibody 24B10, a jumbled arrangement of R7 and R8 growth cones was observed in the medulla (**Fig. 5a–i**; data not shown). Genetic mosaic analyses revealed that targeting defects in R7 were non-cell autonomous (that is, Flamingo protein is not required in the R7 cell for target specificity; data not shown), supporting the idea that defects in R7 projections were a consequence of an earlier role in R8 axons.

To assess how Flamingo contributes to R8 connection specificity, we carried out a detailed study of map formation. In wild-type larvae, axons exited the optic stalk and dispersed at regular intervals along the anterior edge of the lamina (**Fig. 6a**; see also **Figs. 7** and **8d,e**). In contrast to wild-type axons, *fmi* mutant axons dispersed in an irregular fashion (**Fig. 6b**). This disruption in local retinotopic assembly was quantified. In wild type, R8 axon terminals from the anterior-most two columns of ommatidia in the retina penetrated the anterior edge of the lamina, and their number established a 1:1 correspondence between R-cell terminals and ommatidia. In *fmi* mutants, R8 growth cones did not disperse appropriately, reducing this ratio. In wild type, we observed an average R-cell axon terminal:ommatidia ratio of 53:51 ($n = 6$ eye/brain complexes), whereas in *fmi* mutants, the ratio was 25:38 ($n = 5$; $P < 0.005$ using Fisher's Exact Test). Targeted expression of Flamingo in R8 rescued the R8 mutant phenotype (mutant + transgene ratio, 43:40; $n = 4$; **Fig. 6c**). Consistent with a role for *flamingo* in mediating interactions between R8 axons, Flamingo protein showed a transient early burst of expression on R-cell axons in the optic stalk (**Fig. 8b**) and as they entered the optic lobe (**Fig. 8e,f**). Strong labeling was observed in the youngest axons, with decreased expression in more mature axon bundles. The earliest defect detected in the R8 pattern was seen at a stage in development when Flamingo was expressed in R8 axons but not on surrounding cells. These findings support a role for Flamingo in permitting R8 growth cones to separate from each other in an orderly fashion after exiting the optic stalk and entering their target field in the medulla.

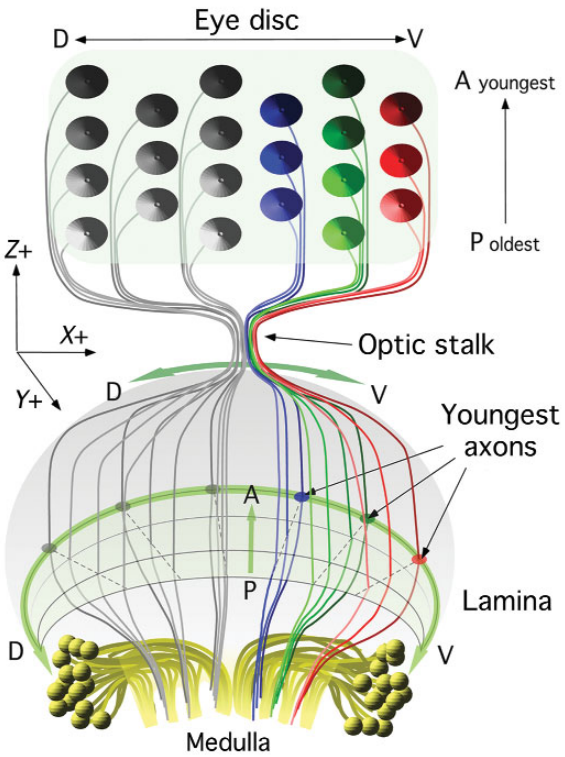

Figure 7 R-cell axons form a topographic map. Diagram highlighting the precise retinotopic arrangement of R-cell axons along the anteroposterior (A–P) and dorsoventral (D–V) axes of the eye disc and optic lobe. There is a direct spatial mapping between the R-cell clusters in the eye disc and the projections of their axons into the optic lobe. The most anterior R cells in the eye disc are the youngest (darkest in color), and their axons form the outermost, leading edge of the crescent-shaped axon array in the lamina. In the rows of R-cell axons innervating the medulla, the youngest axons align most closely with axons of medulla neurons (yellow).

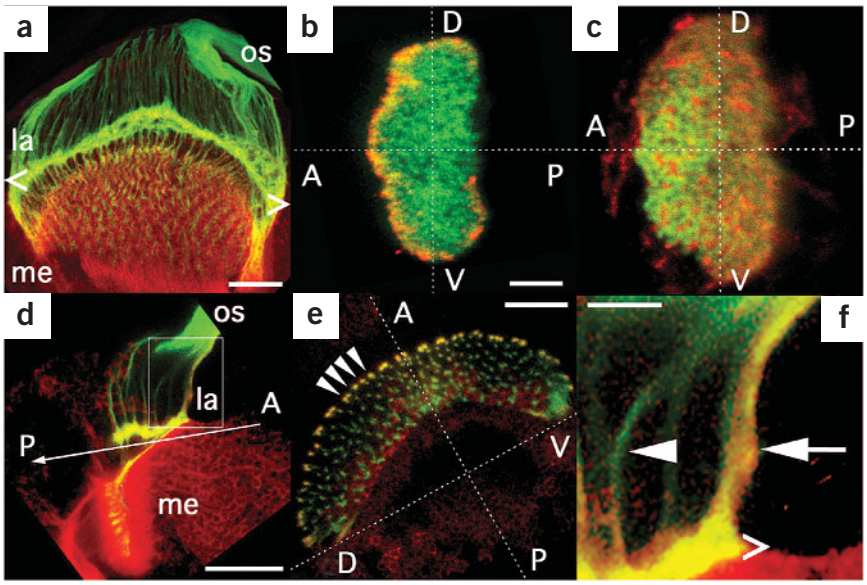

Figure 8 Flamingo protein is transiently expressed in R8 axons as they enter the optic lobe. (**a**,**d**,**f**) The wild-type expression pattern of Flamingo (red) in third-instar larvae, shown relative to R cell–specific expression of GFP (under control of GMR–GFP; green). The lamina is demarcated by brackets (<>). la, lamina; me, medulla; os, optic stalk. (**a**) *En face* view of the R-cell axon array as in **Fig 6**. Note the strong Flamingo expression in the optic lobe beneath the lamina, corresponding to the nascent medulla. (**d**) Lateral view of the R-cell axon array, at a 90° clockwise rotation from the view in **a** about an imaginary *z*-axis running parallel to R-cell axons as they exit the optic stalk and grow toward the lamina. The youngest axons, those from the anterior-most R cells, are towards the right. As axons grow in from newly formed R cells, they displace older axons towards the left. (**f**) Enlarged view of the boxed area in **d** showing Flamingo immunolabelling (yellow) only at the anteriormost edge of the developing lamina, where newly arriving R8 axons project along its outer edge, but above the lamina neuropil (arrow). Flamingo expression on older axons diminishes several rows posterior (arrowhead). (**b**,**c**,**e**) A progression along the path of the photoreceptor axons to their trajectory from the eye disc into the optic lobe. (**b**) Labeling in the optic stalk just prior to entry of axons into the developing optic lobe. Note strong, transient labeling of Flamingo at the periphery of the stalk, the region containing the youngest R8 axons. (**c**) By comparison N-cadherin (red) is expressed throughout the developing optic stalk. (**e**) View of the R-cell axons in the outer crescent lying above the developing lamina plexus at a rotation from **b** of 90° toward the reader about an imaginary axis in the plane of the page. Note transient yellow labeling at the anterior edge of the crescent (arrowheads) revealing transient Flamingo protein expression in R-cell axons. Scale bars (**a**–**c**,**e**), 20 μm; (**d**), 10 μm; (**f**), 5 μm.

DISCUSSION

Our results indicate that the protocadherin Flamingo is crucially involved in regulating target selection in two distinct classes of photoreceptors. In particular, R1–R6 cells lacking *flamingo* function terminate in the correct ganglion, the lamina, but fail to select the appropriate pattern of post-synaptic targets. Within this layer, Flamingo protein expression is largely confined to afferent axons and is highly dynamic during the critical developmental stages when R1–R6 axons are extending to their targets. R8 cells lacking *fmi* function have defects in the local topographic mapping of their terminals. In this context, *fmi* seems to permit R8 growth cones to separate from one another in an orderly fashion as they exit the optic stalk and enter the target field, a phenomenon similar to its role in promoting the appropriate spatial separation of R1–R6 growth cones during target selection in the lamina. Given that Flamingo, like other cadherins, has been shown to mediate homotypic interactions in cell culture, we propose that Flamingo influences R-cell target selection by mediating specific interactions amongst afferent growth cones.

How does Flamingo contribute to the remarkable precision of R1–R6 target specificity? We propose that R1–R6 target selection within the lamina requires three sequential steps, two of which require Flamingo function. First, the orientation of the projection pattern along the dorsoventral axis is set by the orientation of the ommatidium; this is reinforced by a weak dorsoventral signal in the target[20]. Flamingo acts at this early step in the retina to promote the interactions between photoreceptor cell bodies underlying polarity[30,31]. Second, at a later stage in development, Flamingo-mediated interactions between R1–R6 growth cones act prior to axon divergence to define the precise orientation, and hence the extension trajectory, of each growth cone[16,20]. Finally, in a third step, N-cadherin and Lar promote extension toward and/or recognition of specific lamina targets[4,24].

These results leave open several possibilities regarding the precise role of Flamingo in controlling R-cell growth cone trajectory. For example, Flamingo could mediate interactions between R1–R6 growth cones from the same ommatidium, between growth cones of neighboring ommatidia or both. In addition, the observation that Flamingo is strongly expressed by only a subset of R-cell axons at a critical developmental stage raises the possibility that Flamingo might mediate homotypic interactions between specific R-cell growth cones. Indeed, specific interactions between their growth cones are required for R cells to select their correct targets[20]. On the other hand, it remains possible that Flamingo mediates heterotypic interactions with an as-yet unknown ligand, either amongst R-cell growth cones or between these growth cones and their targets. Since Flamingo-related proteins are also expressed within the developing mammalian nervous system[34,35], they may contribute to the formation of specific connections within the mammalian brain through interactions that regulate sorting of growth cones to their appropriate targets.

It is important to note that Flamingo is unlikely to mediate a general or a non-specific adhesive interaction amongst R-cell axons that simply maintains fascicle structure. Indeed, we were unable to detect any changes in the ultrastructural organization of R-cell axon fascicles in animals in which all R-cell axons lack *flamingo* function. As the cues that control the last steps in choosing a synaptic partner are likely to be delivered via cell–cell contact by short-range signals that function by changing growth cone shape and/or position, they are essentially adhesive in nature. Rather than being nonspecific, however, such interactions are likely to be highly regulated with respect to space, time and cell type. Viewed in this context, we find the precise and dynamic regulation of Flamingo expression in R-cell growth cones to be particularly striking.

The orientation process by which R-cell growth cones become polarized prior to extension[1] is broadly similar to the orientation process that underlies the establishment of planar cell polarity in epithelial sheets. In both cases, for example, an underlying rearrangement of the cytoskeleton is likely to be critical. We posit that the role of Flamingo protein in R-cell target selection may be molecularly related to its role in controlling the polarity of ommatidia and, more generally,

of epithelial cells[36]. It is important to note, however, that whereas Flamingo is required for this step, other planar cell polarity genes are not[20], indicating that Flamingo must act with a different, though perhaps overlapping, set of proteins in R-cell growth cones.

Using specific interactions with other R-cells to determine the precise orientation of their growth cones, R-cell axons encounter relatively few potential targets during subsequent extension to their appropriate targets. We suggest that this may reflect a general strategy in which reducing the number of potential targets encountered by an afferent growth cone reduces the requirement for molecular complexity in the cellular recognition events regulating the formation of precise patterns of synaptic connections.

Note added in proof: B. Dickson, T. Uemura and their colleagues have recently also reported that Flamingo is required for the precise connections of R8 in the medulla neuropil (K.A. Senti *et al.*; *Current Biology,* in press).

METHODS

Genetics. Fly stocks were maintained at 22 °C on standard medium and mutagenized using ethylmethane sulfonate following standard procedures. Mosaic flies were generated and tested as previously described using the FRT42D chromosome[24]. The 109(2)68 Gal4 driver was used for R8-specific expression[33].

Immunohistochemistry. Photoreceptor axon projections were examined using mAb24B10 immunolabeling in combination with either HRP/DAB visualization[37] or fluorescent antibody labeling followed by confocal laser scanning microscopy (using a Bio-Rad MRC1024 or a Leica TCS SP2 AOBS)[38].

Electron microscopy. The laminas beneath control and mutant eyes in mosaic flies were prepared for electron microscopy, and single or serial-section profile counts of organelles were made, all as previously reported[39]. Large-area digital montages collected from electron images obtained with a Philips Tecnai 12 by means of a Kodak Megaview II camera and using AnalySIS software (SIS GmbH Münster) were used to derive counts of terminals and synaptic organelles. To assay the regularity of the lamina's cartridge array, cartridges were designated by their centers in cross-sectioned profiles, and the centers of all cartridge profiles were then assigned to the vertices of a mesh connected by DeLaunay triangulation, using software programmed in Matlab (Mathworks).

Behavioral assay. The optomotor response was assayed as previously described[24]. In brief, groups of 20–50 flies were placed at the end of a transparent tube held stationary over a moving pattern of black and white stripes. Flies that can detect the moving stripes orient and move toward the apparent source of motion. Trials last for 1 min and flies that move an arbitrary constant distance toward the source of motion are scored as positive.

Note: Supplementary information is available on the Nature Neuroscience website.

ACKNOWLEDGMENTS

We thank the members of the Zipursky lab and U. Banerjee for comments on the manuscript, and T. Uemura for the anti-Flamingo antibodies. We also thank B. Dickson and T. Uemura for sharing results prior to publication. We thank K. Ronan for assistance in preparing the manuscript, R. Kostyleva for help with EM and J. A. Horne for EM computer methods. This work was supported by postdoctoral fellowships from the Jane Coffin Childs Foundation (T.R.C.), the Burroughs-Wellcome Fund for Biomedical Research (T.R.C.), the Life Science Research Foundation (HHMI) (C.-H.L.), an NIH Medical Scientist Training Program grant (GM08042 to R.L.) and a grant from the National Eye Institute (EY03592 to I.A.M.). I.A.M. is a Guggenheim Fellow; S.L.Z. is an Investigator of the Howard Hughes Medical Institute.

COMPETING INTERESTS STATEMENT

The authors declare that they have no competing financial interests.

Accepted 29 April 2003
Published online 18 May 2003; doi:10.1038/nn1063

1. Tessier-Lavigne, M. & Goodman, C.S. The molecular biology of axon guidance. *Science* **274**, 1123–1133 (1996).
2. Flanagan, J.G. & Vanderhaeghen, P. The ephrins and Eph receptors in neural development. *Annual Review of Neuroscience* **21**, 309–345 (1998).
3. Inoue, A. & Sanes, J.R. Lamina-specific connectivity in the brain: regulation by N-cadherin, neurotrophins, and glycoconjugates. *Science* **276**, 1428–1431 (1997).
4. Lee, C.-H., Herman, T., Clandinin, T.R., Lee, R. & Zipursky, S.L. N-cadherin regulates target specificity in the *Drosophila* visual system. *Neuron* **30**, 437–450 (2001).
5. Yamagata, M., Weiner, J.A. & Sanes, J.R. Sidekicks: synaptic adhesion molecules that promote lamina-specific connectivity in the retina. *Cell* **110**, 649–660 (2002).
6. Huh, G.S. *et al.* Functional requirement for class I MHC in CNS development and plasticity. *Science* **290**, 2155–2159 (2000).
7. Shen, K. & Bargmann, C.I. The immunoglobulin superfamily protein SYG-1 determines the location of specific synapses in *C. elegans*. *Cell* **112**, 619–630 (2003).
8. Schmucker, D. *et al. Drosophila* Dscam is an axon guidance receptor exhibiting extraordinary molecular diversity. *Cell* **101**, 671–684 (2000).
9. Wang, F., Nemes, A., Mendelsohn, M. & Axel, R. Odorant receptors govern the formation of a precise topographic map. *Cell* **93**, 47–60 (1998).
10. Scheiffele, P., Fan, J., Choih, J., Fetter, R. & Serafini, T. Neuroligin expressed in nonneuronal cells triggers presynaptic development in contacting axons. *Cell* **101**, 657–669 (2000).
11. Biederer, T. *et al.* SynCAM, a synaptic adhesion molecule that drives synapse assembly. *Science* **297**, 1525–1531 (2002).
12. Katz, L.C. & Shatz, C.J. Synaptic activity and the construction of cortical circuits. *Science* **274**, 1133–1138 (1996).
13. Crowley, J.C. & Katz, L.C. Development of ocular dominance columns in the absence of retinal input. *Nat. Neurosci.* **2**, 1125–1130 (1999).
14. Lin, D.M. *et al.* Formation of precise connections in the olfactory bulb occurs in the absence of odorant-evoked neuronal activity. *Neuron* **26**, 69–80 (2000).
15. Clandinin, T.R. & Zipursky, S.L. Making connections in the fly visual system. *Neuron* **35**, 827–841 (2002).
16. Meinertzhagen, I.A. & Hanson, T.E. in *The Development of Drosophila melanogaster* (eds. Bate, M. & Martinez-Arias, A.) 1363–1491 (Cold Spring Harbor Press, Cold Spring Harbor, 1993).
17. Kirschfeld, K. Die projektion der optischen unwelt auf das raster der rhabdomere im komplexauge von *Musca*. *Exp. Brain Res.* **3**, 248–270 (1967).
18. Perez, S.E. & Steller, H. Migration of glial cells into retinal axon target field in *Drosophila* melanogaster. *J. Neurobiol.* **30**, 359–573 (1996).
19. Poeck, B., Fischer, S., Gunning, D., Zipursky, S.L. & Salecker, I. Glial cells mediate target layer selection of retinal axons in the developing visual system of *Drosophila*. *Neuron* **29**, 99–113 (2001).
20. Clandinin, T.R. & Zipursky, S.L. Afferent growth cone interactions control synaptic specificity in the *Drosophila* visual system. *Neuron* **28**, 427–436 (2000).
21. Usui, T. *et al.* Flamingo, a seven-pass transmembrane cadherin, regulates planar cell polarity under the control of Frizzled. *Cell* **98**, 585–595 (1999).
22. Chae, J. *et al.* The *Drosophila* tissue polarity gene starry night encodes a member of the protocadherin family. *Development* **126**, 5421–5429 (1999).
23. Gao, F.-B., Kohwi, M., Brenman, J.E., Jan, L.Y. & Jan, Y.N. Control of dendritic field formation in *Drosophila*: the roles of *flamingo* and competition between homologous neurons. *Neuron* **28**, 91–101 (2000).
24. Clandinin, T.R. *et al. Drosophila* LAR regulates R1–R6 and R7 target specificity in the visual system. *Neuron* **32**, 237–248 (2001).
25. Newsome, T.P., Asling, B. & Dickson, B.J. Analysis of *Drosophila* photoreceptor axon guidance in eye-specific mosaics. *Development* **127**, 851–860 (2000).
26. Stark, W.S. & Carlson, S.D. Ultrastructure of capitate projections in the optic neuropil of *Diptera*. *Cell Tissue Res.* **246**, 481–486 (1986).
27. Meinertzhagen, I.A. & O'Neil, S.D. Synaptic organization of columnar elements in the lamina of the wild type in *Drosophila melanogaster*. *J. Comp. Neurol.* **305**, 232–263 (1991).
28. Meinertzhagen, I.A. & Sorra, K.E. Synaptic organization in the fly's optic lamina: few cells, many synapses and divergent microcircuits. *Prog. Brain Res.* **131**, 53–69 (2001).
29. Fröhlich, A. & Meinertzhagen, I.A. Cell recognition during synaptogenesis is revealed after temperature-shock-induced perturbations in the developing fly's optic lamina. *J. Neurobiol.* **24**, 1642–1654 (1993).
30. Yang, C.-H., Axelrod, J.D. & Simon, M.A. Regulation of Frizzled by fat-like cadherins during planar polarity signaling in the *Drosophila* compound eye. *Cell* **108**, 675–688 (2002).
31. Das, G., Reynolds-Kenneally, J. & Mlodzik, M. The atypical cadherin Flamingo links Frizzled and Notch signaling in planar polarity establishment in the *Drosophila* eye. *Dev. Cell.* **2**, 655–666 (2002).
32. Brand, A.H. & Perrimon, N. Targeted gene expression as a means of altering cell fates and generating dominant phenotypes. *Development* **118**, 401–415 (1993).
33. White, N.M. & Jarman, A.P. *Drosophila* atonal controls photoreceptor R8-specific properties and modulates both receptor tyrosine kinase and Hedgehog signaling. *Development* **127**, 1681–1689 (2000).
34. Formstone, C.J. & Little, P.F.R. The *flamingo*-related mouse *Celsr* family (*Celsr1-3*) genes exhibit distinct patterns of expression during embryonic development. *Mech. Dev.* **109**, 91–94 (2001).
35. Tissir, F., De-Backer, O., Goffinet, A.M. & Lambert de Rouvroit, C. Developmental expression profiles of Celsr (Flamingo) genes in the mouse. *Mech. Dev.* **112**, 157–160 (2002).
36. Adler, P.N. Planar signaling and morphogenesis in *Drosophila*. *Dev. Cell* **2**, 525–535 (2002).
37. Martin, K.A. *et al.* Mutations disrupting neuronal connectivity in the *Drosophila* visual system. *Neuron* **14**, 229–240 (1995).
38. Garrity, P.A. *et al.* Retinal axon target selection in *Drosophila* is controlled by a receptor protein tyrosine phosphatase. *Neuron* **22,** 707–717 (1999).
39. Meinertzhagen, I.A. Ultrastructure and quantification of synapses in the insect nervous system. *J. Neurosci. Methods* **69**, 59–73 (1996).